
Article

Temporal and spatial dynamics of drought in Central Asia during 2002-2017 based on GRACE Data

Keting Feng¹, Yaonan Zhang^{1,*}, Yanping Cao² and Yongping Shen¹

¹ National Glaciology Geocryology Desert Data Center, Northwest Institute of Eco-Environment and Resources, Chinese Academy of Sciences, Lanzhou 730000, China; fengkt@lzb.ac.cn; shenyp@lzb.ac.cn

² College of Geography and Environmental Science, Henan University, Kaifeng 475004, China; caoy@lzb.ac.cn

* Correspondence: fengkt@lzb.ac.cn; yaonan@lzb.ac.cn

Abstract: With the influences of climate change and human activities, the resources and environment of “One Belt and One Road” are facing severe problems and challenges. This study aims to analyze the temporal and spatial dynamics of the drought environment and the response of vegetation cover to the drought by using drought indicators. Gravity Recovery and Climate Experiment (GRACE) drought severity index (GRACE-DSI) and GRACE water storage deficit index (GRACE-WSDI), were calculated to present hydrological drought. Moreover, based on GRACE, Water-Global Assessment and Prognosis (WaterGAP) model, and Global Land Data Assimilation System (GLDAS) data, the groundwater in Central Asia was retrieved to calculate the groundwater drought index called the GRACE Standardized Groundwater Level Index (GRACE-SGI). The results show that the annual precipitation in Central Asia increased slightly at a rate of 0.39 mm/year ($p = 0.82$) since 2000, while the temperature increased slightly at a rate of 0.05 °C/year ($p = 0.10$). The water storage decreased significantly at -0.59 mm/year ($p < 0.01$) and experienced a decrease-increase-decrease process. During the study period, the arid situation in Central Asia deteriorated, especially in the eastern coast of the Caspian Sea and the Aral Sea basin. From 2007 to 2015, the Central Asian environment was generally arid and suffered from different durations and degrees of hydrological and groundwater droughts. The drought indicators (i.e., GRACE-DSI, GRACE-WSDI) and the NDVI showed a significantly positive correlation during the growing season. However, the NDVI of cultivated land and grassland distribution areas in Central Asia showed a strong negative correlation with GRACE-SGI. It is concluded that the drought environment in Central Asia affected the growth of vegetation. The continued deterioration of the arid situation may further stress the ecological system in Central Asia.

Keywords: Central Asia; GRACE; drought; vegetation; water storage; groundwater

1. Introduction

Drought is the most common and the most widespread natural disaster in the world. It can be frequent and long-lasting, resulting in a wide range of impacts and damages. Drought has a profound impact on agricultural production, ecological environment, and socio-economic development [1]. The economic losses caused by global climatic disasters account for 70% of total losses of natural disasters, while the losses resulting from drought account for 50% of the climatic losses [2]. Climate change is still a global challenge as poorly addressed by governments, and climate warming made drought disasters and risks more and more severe [3]. Unfortunately, the occurrence of global drought disasters has gradually become overwhelming as the frequency and intensity of extreme drought events continue to increase. Drought disasters became more prominent and more destructive, and their impacts lead to global consequences [4]. While causing huge economic losses, droughts also increasingly have an enormous negative impact on society and the ecological environment, especially in developing countries. In addition, human activities

contributed to the accelerating droughts, especially in arid and semi-arid regions, where natural ecosystems are relatively vulnerable, with a combination of low rainfall, intensive evaporation, low vegetation covers, and scarce water resources. The drought occurrences in human-dominated environments should not be perceived as purely natural hazards since anthropogenic changes to the land surface alter hydrological processes and affect the development of drought [5]. Meteorological to hydrological drought propagation was influenced mostly by direct human activities, which has both positive and negative effects on the severity and duration [6].

Central Asia is located in the core area of "One Belt and One Road", and is an inland arid and semi-arid region, with extremely unevenly distributed water resources [7, 8]. Municipal and industrial water sources are mainly sourced from glacial meltwater, which somewhat alleviates the drought stress in Central Asia [9]. Due to significant geographic heterogeneity and complex climate system processes [10], ecosystems are very sensitive to global climate changes [11]. In the past 30 years, the temperature rise rate in Central Asia reached 0.4 °C/decade, higher than that of the northern hemisphere land and surrounding areas (0.3 °C/decade). Moreover, it shows rapid warming in the center of Central Asia, while a decreasing rate from northwest to southeast [12]. The changing climate impacts the water resources in the region directly and rapidly. The total water storage over Central Asia, derived from GRACE and GLDAS, shows a decreasing trend over the past 30 years [13]. The water resources diminished from 2003 to 2013 at a rate of -4.44 ± 2.2 mm/a [14].

Climate change and its environmental pressure on the unique temperate desert ecosystems of Central Asia threaten the ecological security of the core area of "One Belt and One Road". With the background of global warming, there have been significant vegetation changes in Central Asia since the 21st century. While vegetation greening led to significant temperature decreasing, that moderating regional warming throughout Central Asia [15], the arid environment in Central Asia is getting drier [16]. Between 1966 and 2015, most drought events in Central Asia lasted 3 to 5 months and tended to have an east-west trajectory [17]. Since the beginning of the 21st century, Kazakhstan suffered drought hazards every year. Droughts in different severity occurred in half of Central Asia in 2000, 2008, 2011, 2012, and 2014, and the most severe droughts took place in 2012 and 2014 [18]. Due to the combination of low rainfall, high temperature, and frequent natural disasters, western Central Asia's desertification is intensifying [19]. In the future century, Central Asia is expected to become drier, especially in the western part of Turkmenistan, Uzbekistan, and Kazakhstan, potentially impacting agriculture in the region [20].

Traditionally, the drought monitoring and evaluation methods are mostly based on hydrometeorological observation data, such as precipitation and evapotranspiration. Due to the spatial heterogeneity of the natural environment and the scarcity of ground-based observations, the spatial distribution characteristics of droughts obtained through interpolation have large uncertainties [21], which necessitates further improvements. Additionally, it is infeasible to adequately assess the risk of drought disasters based on a single variable or indicator, such as precipitation, runoff, or soil water [22]. The causes and effects of droughts are complex, affecting not only surface water but also groundwater. Changes in regional-scale water storage include groundwater, soil water, surface water, ice, snow, biological water content, precipitation, evapotranspiration, and so on.

Hence, the drought indicators that consider all of these changes can more comprehensively capture the characteristics of drought disasters. The Gravity Recovery and Climate Experiment (GRACE) satellites are used to monitor the dynamics of terrestrial water storage [23], and the hydrological variations [24]. The change in water storage derived by the GRACE satellites, including surface water and the groundwater over 10 km, is the composite outcome of natural processes and human activities. The analysis of droughts from GRACE-based water storage is more comprehensive than the traditional methods [25]. Comparing to other remote sensing data for monitoring the occurrence of droughts, GRACE assessments of water storage have the advantage of predicting hidden drought disasters. For example, the soil moisture in the root zone may be in a suitable condition,

while irrigated agriculture consumed a large amount of groundwater. Thus, GRACE assessments of water storage are valuable for monitoring and predicting drought disasters.

Based on the gridded hydrological drought index and groundwater drought index retrieved from GRACE satellite water storage changes, this paper quantitatively evaluates the spatial and temporal distribution of hydrological and groundwater drought events in Central Asia since the 21st century. This study could provide scientific data for the eco-environmental protection policies and practices.

2. Materials and Methods

2.1. Study Area

The Central Asian region (35.14°~ 55.44°N, 46.50°~ 87.35°E) includes five countries: Kazakhstan, Kyrgyzstan, Tajikistan, Uzbekistan, and Turkmenistan. It is located in the Eurasian continent's hinterland, covering a vast area of about 4.19 million km² (Figure 1). The terrain is generally high in the southeast and low in the northwest, with a typical mountain basin structure. The region is of a typical continental climate of temperate deserts and grasslands, with sparse and extremely uneven distributed precipitation (125 to 289 mm/year) [26], and climate is drier in the east and west than the rest. The average summer (July) temperature is between 26°C and 32°C, while temperature ranges from -20°C at the northern end to 2°C in the south of the basin. The regional evapotranspiration greatly exceeds precipitation. As shown in Fig. 1, the major vegetation types in Central Asia are cropland (22%), grassland (24%), forest (2%), shrubs (7%) and sparse vegetation (17%). The southeast parts of Central Asia are mainly mountainous areas, with abundant water resources. Central Asia's center is mainly covered by sparse vegetation; the northern CA is dominated by farmland and grassland, while grasslands and croplands are mixed in the eastern part. The mountain-oasis-desert ecosystem in this area makes it unique and complex in response to global climate change [27].

Central Asia has rich land resources; however, local agriculture is not fully developed due to the limitation of water resources. The per capita arable land area of the five Central Asian countries is 0.52 hectares, which is about six-fold of the one in China. Agriculture is the primary sector in Central Asia; about 90 % of water abstractions are consumed in local agriculture, with the land undergoing widespread irrigation [28]. According to the FAO statistics, irrigated agriculture prevails in Central Asia except for the northern part of Kazakhstan, where features rainfed agriculture (<http://www.fao.org/nr/water/aquastat/irrigationmap/index10.stm>). Given the necessity for irrigation across most of Central Asia, water is the most critical factor driving the economic and social development in the region [29].

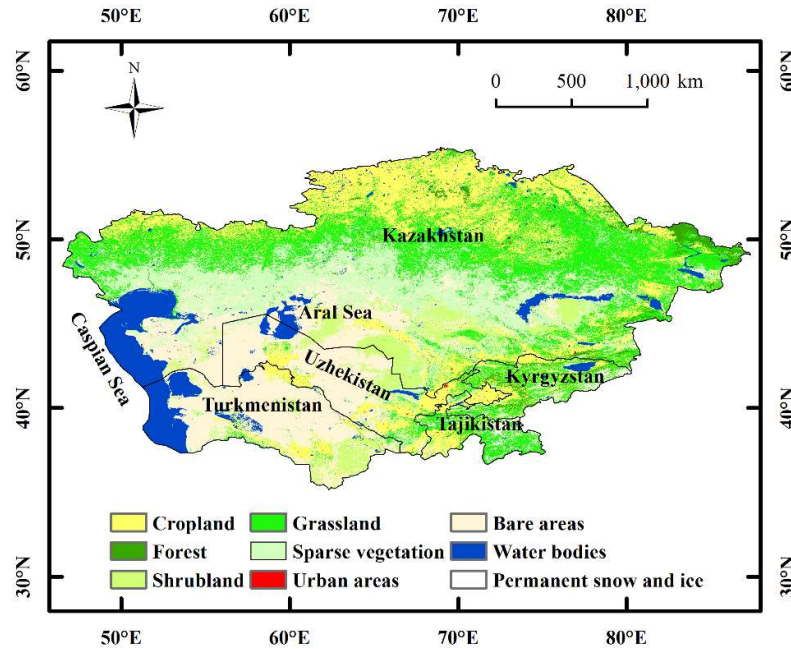


Figure 1. The location of the Central Asia, and land cover over the Central Asia in 2018. The Central Asia includes five countries.

2.2. Satellite Data

GRACE satellites launched in 2002 provide a new method to monitor drought/flood events. Terrestrial water storage changes (TWSC) can be captured by GRACE satellites observing Earth's mass redistribution. The latest GRACE CSR RL06 Mascon TWSC were retrieved via the GRACE website (http://www2.csr.utexas.edu/grace/RL06_mascons.html). This dataset has a monthly temporal resolution and a spatial resolution of 0.25° . Previous studies have shown that the accuracy of the TWSC based on the Mascon algorithm is higher [30]. The terrestrial water storage anomalies (TWSA) were calculated by removing the monthly average of TWSC during the study period from the monthly TWSC. Previous studies that focused on the spatiotemporal characteristics of TWSC of Central Asia [13, 14] approved the effectiveness of GRACE data in this region. With the support of TWSA, we calculated two hydrological drought indicators, the GRACE drought severity index (GRACE-DSI) [31] and the GRACE water storage deficit index (GRACE-WSDI) [32].

The GRACE TWSC integrates five parts, including groundwater, soil water, surface water, ice and snow water, and biological water content in the vertical direction [33]. Biological water change is usually neglected due to its relatively little change amount in deriving groundwater change [34]. With the availability of the GRACE TWSA, the soil moisture and snow water equivalent data of the Global Land Data Assimilation System (GLDAS), surface water storage of the hydrological model Water-Global Assessment and Prognosis (WaterGAP), we derive the groundwater storage in Central Asia by Equation 1. Further, the GRACE standardized groundwater level index (GRACE-SGI) [35] is calculated accordingly.

$$\Delta GWS = TWSA - \Delta SM - \Delta SWE - \Delta SW \quad (1)$$

where Δ represents the amount of change, GWS is the groundwater storage, TWSA is the terrestrial water storage anomalies, SM is the soil moisture, SWE is the snow water equivalent, and SW is the surface water.

The soil moisture (SM), snow water equivalent (SWE), precipitation, and air temperature were obtained from the Noah model of GLDAS-2.0 and GLDAS-2.1 [36], at the monthly time scale with a spatial resolution of $0.25^\circ \times 0.25^\circ$. The GLDAS model data have been widely used in various regions, including Central Asia [13, 14]. All of the spatial data

were reprojected to the WGS84 geographic coordinate system and were masked by the study area's boundary. Based on the monthly soil moisture and snow water equivalents, the monthly anomalies between 2002 and 2017 were calculated, which is the monthly values of soil moisture or snow water equivalent minus the averages. Based on the principle of groundwater-derived, the spatial and temporal dynamics of groundwater in the region were quantitatively retrieved with water storage change, soil moisture, and SWE anomalies. The climate distribution in Central Asia was analyzed, and the gridded Standard Precipitation Index (SPI) at different periods were calculated with monthly precipitation [37].

The surface water storage, including rivers, lakes, wetlands and reservoirs, were obtained from the hydrological model WaterGAP, which was developed by Döll et al. [38]. This model simulates global-scale terrestrial water storages and flows under the influence of humans except Antarctica [38, 39]. With a spatial resolution of $0.5^\circ \times 0.5^\circ$ every month, surface water storage from WaterGAP model for the period of 2003-2016 were used in this paper. A thorough description of the model and its components can be found in Müller Schmied et al. [39].

The surface water storage, including rivers, lakes, wetlands and reservoirs, were obtained from the hydrological model WaterGAP [38]. This model simulates global-scale terrestrial water storages and flows under the human influence [38, 39]. Monthly surface water storage from WaterGAP model for 2003-2016 is in a spatial resolution of $0.5^\circ \times 0.5^\circ$. A thorough description of the model and its components is available in Müller [39].

We utilized the L3 level normalized vegetation index (NDVI) at 0.05° spatial resolution of the Terra Moderate Resolution Imaging Spectroradiometer (MODIS) sensor (MODIS / Terra Vegetation Indices Monthly L3 Global 0.05° CMG) from 2002 to 2017 derived from the NASA Land Processes Distributed Active Archive Center (LPDAAC) (available at <https://ladsweb.modaps.eosdis.nasa.gov/search/>). The MODIS Reprojection Tools (MRT) was used to implement the format conversion, splicing, and projection.

With the support of python and the arcpy package, the 0.5° grid surface water and 0.05° grid NDVI index data were resampled to 0.25° resolution.

Renewable water resources per capita in the five Central Asia countries were obtained from the website (<https://www.worldometers.info/water/>). Here the "renewable water source" refers to the water resource removed from a lake or river. A portion of this water is often returned to the source and is available again; therefore, this source is termed "renewable water source". For more detailed information, please refer to the website data description.

2.3. Data analysis

2.3.1. Drought indexes

This study calculated GRACE-DSI, GRACE-WSDI and GRACE-SGI based on the changes in the water content of a grid. For each grid, the standardized anomalies of GRACE TWSA for month j and year i (ranging from 2002 to 2017), as $DSI_{i,j} = \frac{TWSA_{i,j} - \overline{TWSA_j}}{\sigma_j}$, where σ_j and $TWSA_j$ are the standard deviation and average value of TWSA for j -month, respectively [31]. The global GRACE-DSI distribution meets the non-standard state distribution. Table 1 lists the classification of different classes of drought according to GRACE-DSI.

Table 1. Dynamic range and relative categories for dry conditions of GRACE-DSI, GRACE-WSDI, GRACE-SGI and SPI.

Category	Description	GRACE-DSI	GRACE-WSDI	GRACE-SGI	SPI
D0	Near normal	0.49 to -0.49	0 or greater	-0.3 or greater	-0.5 or greater
D1	Mild dry	-0.50 to -0.79	-1.0 to 0	-0.6 to -0.3	-1.0 to -0.5
D2	Moderate drought	-0.80 to -1.29	-2.0 to -1.0	-0.9 to -0.6	-1.5 to -1.0
D3	Severe drought	-1.30 to -1.59	-3.0 to -2.0	-1.2 to -0.9	-2.0 to -1.5
D4	Extreme drought	-1.60 to -1.99	-3.0 or less	-1.5 to -1.2	-2.0 or less
D5	Exceptional drought	-2.0 or less		-1.5 or less	

GRACE-WSDI [32] is able to identify various levels of hydrological drought events, with following equation.

$$WSD_{i,j} = TWSA_{i,j} - \overline{TWSA_j} \quad (2)$$

$$WSDI_{i,j} = \frac{WSD_{i,j} - \mu}{\sigma} \quad (3)$$

where $\overline{TWSA_j}$ refers to the average TWSI of j-months from 2002 to 2017. and refer to the mean value and standard error of the WSD time series data, respectively. The Table 1 lists the classification of different degrees of drought according to GRACE-WSDI. Based on the standard normal distribution, the GRACE-WSDI values between great than 0, -1.0 and 0, -2.0 and -1.0, -3.0 and -2.0, less than -3.0 are classified as near normal, mild dry, moderate drought, severe drought and extreme drought, respectively.

GRACE-DSI and GRACE-WSDI are mainly used to assess hydrological drought events. When extreme hydrological drought occurs, groundwater drought events also occur when groundwater resources are severely depleted. Based on the GRACE inversion of grid-scale groundwater data, the groundwater drought assessment index GRACE-SGI [35] is calculated via Equation 4:

$$SGI_{i,j} = \frac{\Delta GW_{i,j} - \overline{\Delta GWS}}{\sigma_{\Delta GWS}} \quad (4)$$

SPI is a commonly used indicator for assessing drought disasters based on precipitation alone [40]. Since the distribution of precipitation is asymmetric, when analyzing drought disasters based on precipitation, the gamma function Γ describes the change in precipitation. After calculating the Γ probability distribution in a certain period, the standard normalization processing is performed, and the drought level is finally classified by the cumulative frequency distribution of precipitation. Assuming that the amount of precipitation in a certain period is x , its probability density function (PDF) is shown in Equation 5:

$$f(x) = \frac{1}{\beta^\alpha \Gamma(\alpha)} x^{\alpha-1} e^{-\frac{x}{\beta}}, \quad x > 0 \quad (5)$$

Where α and β are shape parameters and scales respectively, $\alpha > 0$, $\beta > 0$; x is the amount of precipitation; $\Gamma(x)$ is the gamma function. α and β can be obtained by the maximum likelihood estimation method, according to Equation 6 and 7:

$$\alpha = \frac{1}{4A} \left(1 + \sqrt{1 + \frac{4A}{3}} \right) \quad (6)$$

$$\beta = \frac{\bar{x}}{\alpha} \quad (7)$$

where $A = \ln(\bar{x}) - \frac{\sum \ln(x)}{n}$, n is the length of the measured precipitation and the specific calculation steps follows McKee et al. [37].

The monthly SPI is calculated based on the precipitation of the previous i months. The specific period length is i . The i could be equal to 1, 3, 6, 9, 12, 24, and 36. When i is 1 or 3, it is a short-term drought, 6 and 9 represent medium-term droughts, and 12, 24 and 36 mean long-term droughts. The short-term SPI reflects the drought upon agriculture in the short term, such as deficit of soil moisture, crop yield reduction, etc. Long-term SPI reflects the droughts in hydrology and water supply, such as reducing groundwater, runoff, and reservoir water storage [41]. Table 1 lists the classification of drought levels according to GRACE-DSI, GRACE-WSDI, GRACE-SGI and SPI [31, 32, 42, 43].

2.3.2. Linear regression analysis

The spatial-temporal dynamics of the arid environment (drought index) and climate (precipitation and temperature) in Central Asia were analyzed with univariate linear regression. The rate of change of TWSA, drought indexes (i.e., DSI, WSDI and SGI) was calculated respectively by Equation 3 [44].

Many statistical methods are available to measure time series trends; we estimated the significance of change trends based on the p-value.

2.3.3. Correlation analysis

The correlation coefficient can quantitatively describe the strength of the linear relationship between two variables. For two variables x and y , if their sample values are x_i and y_i ($i = 1, 2, \dots, n$), the correlation coefficient between them is defined as Equation 8:

$$r_{x,y} = \frac{\sum_{i=1}^n (x_i - \bar{x})(y_i - \bar{y})}{\sqrt{\sum_{i=1}^n (x_i - \bar{x})^2 \times \sum_{i=1}^n (y_i - \bar{y})^2}} \quad (8)$$

where \bar{x} and \bar{y} represent the average of the sample values of the two variables.

We calculated two correlation coefficients; the one between GRACE drought index and SPI, and the one between GRRACE and NDVI. The value of r can range from -1 to 1. Positive values indicate a positive correlation, and vice versa, 0 means no correlation. The non-parametric Mann-Kendall trend test method [45] was applied to determine the changing trend at the confidence level of 95%.

3. Results and discussion

3.1. Temporal Distribution of the Climate in Central Asia

Central Asia is a climate-sensitive area. From 1901 to 2013, the seasonal precipitation in Central Asia concentrated in spring and summer, while the spring precipitation was predominant. The monthly precipitation in spring and winter increased, while the precipitation in summer and autumn gradually decreased [46]. The analysis of the GLDAS Noah model's precipitation and temperature data (Figure 2) indicates that precipitation and temperature in Central Asia increased slightly since 2000. The annual precipitation increased at a rate of 0.39 mm / year ($p = 0.82$), and the annual mean temperature has increased at a rate of 0.05 °C / year ($p = 0.10$). However, the strong interannual variation of both variables existed in the period. The maximum and minimum precipitation was recorded in 2015 and 2008, respectively, while the highest and lowest mean temperature was recorded in 2013 and 2001, respectively. Figure 2(b) and 2(d) illustrate significant seasonal variations of precipitation and temperature of the region. Precipitation concentrated in the Spring (March-May), accounting for 30.3% of the annual precipitation approximately. The peak precipitation occurred in March and the lowest was in September. The highest temperature of the year occurred in July, and the coldest temperature was in January.

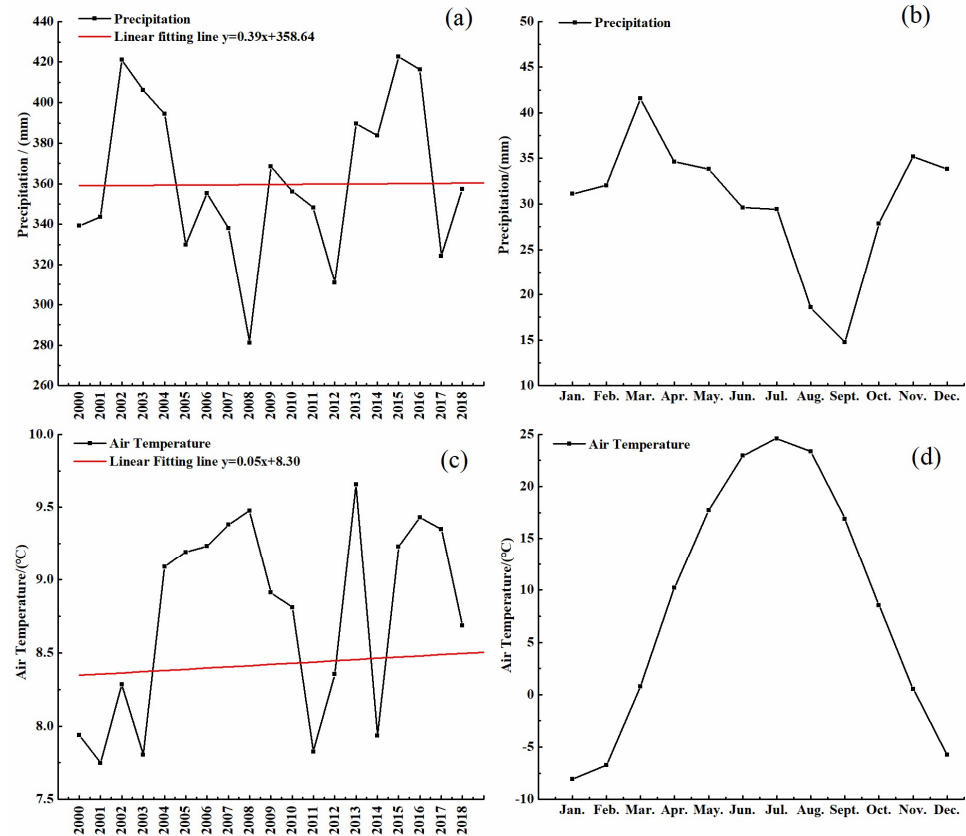


Figure 2. Changes in precipitation (a) and temperature (c), and multi-year monthly precipitation (b) and temperature (d) in Central Asia from 2000-2017.

3.2. Spatial and temporal distribution of water resources in Central Asia

Since 2000, increased precipitation, rising temperatures, and human interference have changed Central Asia's water resources [14]. As shown in Figure 3, in the context of climate change and human activities, the water resources per capita in the five Central Asia countries were decreasing year by year. Figure 4 demonstrates the significant seasonal changes in water storage from 2002 to 2017 in Central Asia; the peak was around April of each year, and the low value was around October of each year. Comparison Figure 4 with Figure 2(b) indicated that the seasonality of water storage is consistent with precipitation, while the change in water resources lagged by a month. The quarterly dynamics of the water resources followed the variable precipitation. The monthly TWSA ranged from -98.96 mm to 96.18 mm, with a peak in April 2005 and the minimum in September 2015. From April 2002 to April 2005, the total regional water storage showed an upward trend with a rate of 0.99 mm/year ($p < 0.09$). However, it showed a significant downward trend from April 2005 to September 2015 with a rate of -0.65 mm/year ($p < 0.01$). Then, from September 2015 to June 2017, it showed a significant upward trend with a change rate of 4.38 mm/year ($p < 0.01$). Since 2000, the Central Asian water storage has fluctuated over time. Over the entire study period, the total regional water storage showed a significant downward trend with a rate of -0.59 mm/year ($p < 0.01$).

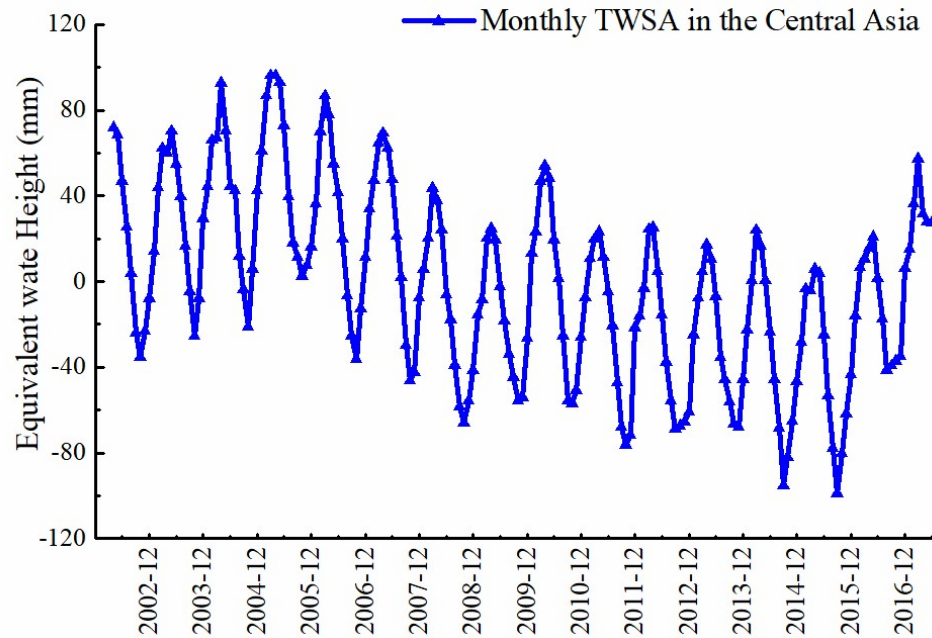


Figure 3. Monthly Total Water Storage Anomaly (TWSA) in the Central Asia from April 2002 through June 2017.

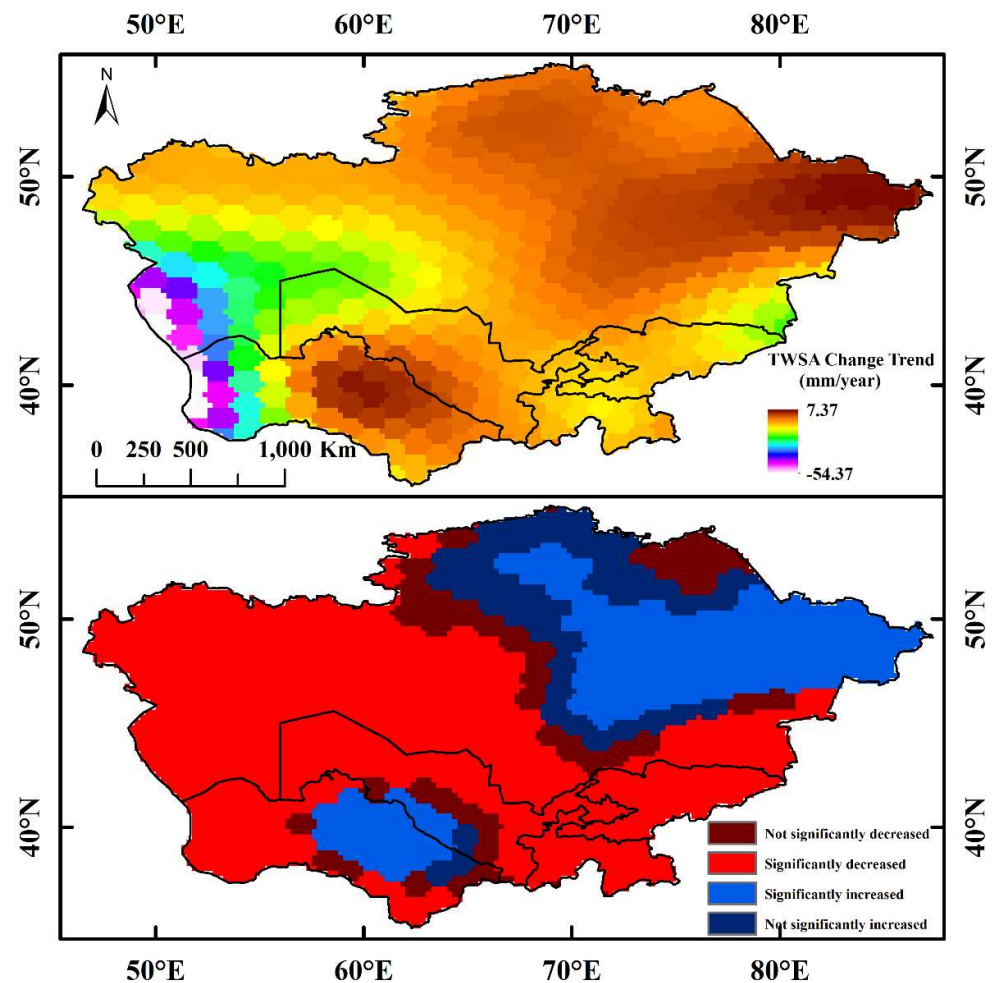


Figure 4. Temporal and spatial trend of total water storage in Central Asia from 2002-2017.

Regarding the spatially change rate (Figure 4), water storage change from 2002 to 2017 had evident spatial heterogeneity. The change rate of all grids varied between -54.37 mm/year to 7.37mm/year, while 56.22% of the area showed a significant downward trend, mainly in the western and southeastern regions of Central Asia. The declining trend of the water storage in the western region was the largest; 21.14% of the area had a significant increasing trend, mainly in Central Asia's northeast and southwest regions. These results indicated that Central Asia's water storage decreased in the western regions while increased in the eastern. The significant water storage reduction in the entire region was mainly due to the rapid decrease in the western region. Previous studies argued that human activity was the main reason for the rapid decline in water reserves in Central Asia's western region [14].

3.3. Correlation analysis between GRACE drought indexes and SPI indexes

Droughts are very likely to occur with the background of severe shortages of regional water resources in Central Asia. Previous studies showed that the SPI drought index is a significant indicator for monitoring long-term hydrological drought events [47]. We firstly investigated the relationship among GRACE hydrological drought indicators (DSI, WDSI), groundwater drought indicators (SGI), and SPI drought indicators. We utilized the comparative analysis to identify the drought events in Central Asia since 2000, and the dry/wet environment. The correlation coefficients between the average of the three indicators (GRACE-DSI, GRACE-WDSI, and GRACE-SGI) and the SPI for different periods were calculated in the entire Central Asia region (Table 2). In Table 2, the correlation coefficients between the GRACE-DSI and SPI indicators are the same as the correlation coefficients between the GRACE-WDSI and SPI, indicating a similarity between GRACE-DSI and GRACE-WDSI. The correlation coefficients between GRACE-DSI, GRACE-WDSI, and SPI values range between 0.05 and 0.72 over different periods and gradually increase with time. The correlation coefficients of GRACE-DSI, GRACE-WDSI and SPI-36 reach 0.72, indicating that GRACE hydrological drought indicators are sensitive to long-term hydrological drought events. The correlation coefficient between SPI and GRACE-DSI and GRACE-WDSI are more significant than the correlation coefficient between SPI and GRACE-SGI. The correlation coefficients are mainly distributed between -0.45 and 0.08, and only the correlation coefficient between GRACE-SGI and SPI-36 is positive, with a value of 0.08. Overall, the correlation between GRACE-SGI and each SPI indicator is insignificant.

Table 2. Average correlations between GRACE DSI, WDSI, SGI and SPI for different accumulation periods.

SPI	DSI	WDSI	SGI
SPI1	0.05	0.06	-0.22
SPI3	0.22	0.22	-0.32
SPI6	0.32	0.31	-0.37
SPI9	0.38	0.38	-0.36
SPI12	0.45	0.44	-0.28
SPI24	0.64	0.64	-0.09
SPI36	0.72	0.72	0.19

The further analysis revealed the spatially distributed correlation coefficients between GRACE-DSI, GRACE-WDSI, GRACE-SGI and SPI-1, SPI-3, SPI-6, SPI-9, SPI-12, SPI-24, SPI-36. In Figure 5 and Table 3, the correlations between GRACE-DSI, GRACE-WDSI, and SPI indicators have similar patterns, mainly with significant positive correlations. As the SPI time scale increases, the area with positive correlations increases, ranging from 74.08% to 92.90%. Intensely positive correlation grids concentrated in Kazakhstan's western and northern regions, and the other regions are mainly weakly negatively correlated. The negative correlation coefficient is relatively strong in Turkmenistan's central

region and Uzbekistan-Kazakhstan's central junction. Nevertheless, with the increase of the SPI time scale, the spatial correlation coefficients show an increasing trend.

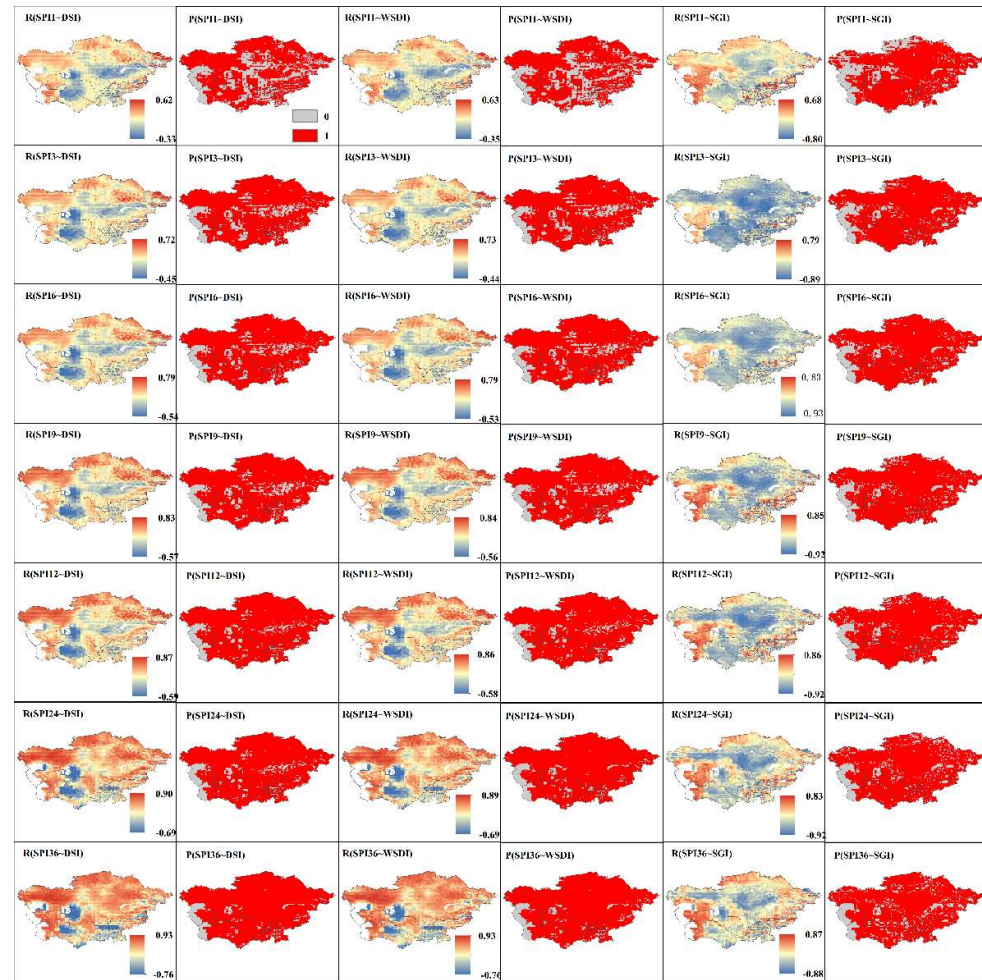


Figure 5. Spatial correlation coefficients between GRACE-DSI, WSDI, SGI and SPI during 2002-2017.

Table 3. Percentage of pixels with positive or negative correlation and mean correlation between the GRACE drought indexes and SPI indexes.

	DSI			WSDI			SGI		
	>0	<0	Mean	>0	<0	Mean	>0	<0	Mean
SPI1	74.08	25.92	0.05	73.91	26.09	0.06	17.59	82.41	-0.22
SPI3	86.62	13.38	0.22	86.46	13.54	0.22	15.95	84.05	-0.32
SPI6	86.86	13.14	0.32	86.87	13.13	0.31	17.12	82.88	-0.37
SPI9	86.92	13.08	0.38	86.84	13.16	0.38	19.71	80.29	-0.36
SPI12	89.64	10.36	0.45	89.52	10.48	0.44	23.43	76.57	-0.28
SPI24	91.43	8.57	0.64	91.17	8.83	0.64	33.32	66.68	-0.09
SPI36	92.90	7.10	0.72	92.88	7.12	0.72	46.37	53.63	0.19

Unlike the relationship between GRACE-DSI and GRACE-WSDI indicators, the GRACE-SGI index and the SPI indexes are mainly negatively correlated. Among the correlation coefficients between the GRACE-SGI and SPI-1, 86.03% of the area are correlated negatively. The negatively correlated regions decrease with the increase of the SPI time scale. Among the correlation coefficients between GRACE-SGI and SPI-36, 56.81% of the area are negatively correlated. The area with strong negative correlations (up to -0.93) is mainly distributed in Kazakhstan's central and western regions and the central and

eastern regions of Uzbekistan and Turkmenistan. The strong positive correlations (up to 0.89) are located mainly in Western Kazakhstan and Western Turkmenistan. There are active dynamic changes in groundwater resources in Central Asia. The strong negative correlation between GRACE-SGI and SPI indicates that although the regional precipitation shows an increasing trend, the groundwater resources are severely depleted, and its consumption is more extensive than precipitation recharge. The strong positive correlation between GRACE-SGI and SPI, on the other hand, indicates that regional dynamic changes in groundwater are consistent with precipitation changes. According to the land use/land cover in Central Asia, the areas with a significant negative correlation between GRACE-SGI and SPI are mainly distributed in grassland areas, while the area with a significant positive correlation are found in areas of bare land. The findings imply that the precipitation is insufficient to meet the water demand for grassland growth in Central Asia, which requires supplementary groundwater. On the other hand, the amount of precipitation in bare areas can fully recharge the groundwater resources.

3.4. Spatiotemporal distribution of drought conditions in Central Asia

The strong correlation between the GRACE drought indicators and the SPI drought indicators for different periods indicates GRACE drought indicators' effectiveness. According to GRACE's drought indicator category, this study only analyzed mild drought events that last for three months or more, and the drought disasters above moderate drought.

According to the GRACE drought indicators in Central Asia, since 2000 the mild droughts have been the predominant events, the moderate droughts have been relatively infrequent, and no extreme drought disasters occurred. Based on the GRACE-DSI indicator, seven mild drought events and four moderate drought events occurred from April 2002 to June 2017. Based on the GRACE-WSDI drought indicator, four mild droughts and two moderate droughts occurred. Based on the GRACE-SGI index, there were 4 mild drought periods, six moderate droughts, and three severe droughts. Although the results differ among indicators, GRACE-DSI is similar to GRACE-WSDI, which is sensitive to regional hydrological droughts. GRACE-SGI is more sensitive to drought events due to insufficient groundwater resources. The Central Asia region was relatively dry during 2007-2015, and there were many consecutive hydrological droughts and groundwater droughts in different periods (Table 4). The annual precipitation from 2005 to 2013 continued to be deficient, while temperature continued to be high. The combination of low precipitation and high temperature in the period is the fundamental reason for the shortage of water resources and drought in Central Asia. Guo et al.[17] calculated the Standardized Precipitation Evapotranspiration Index (SPEI) in Central Asia from 1966 to 2015 and identified drought events in that period. Four of the drought events in April 2008 to August 2008, March 2009 to August 2009, June 2010 to February 2011 and December 2013 to September 2014) are consistent with our results of GRACE-DSI and GRACE-WSDI, and one period (December 2013 to September 2014) is consistent with the result from GRACE-SGI.

Table 4. Distribution of drought disasters in Central Asia.

	Light drought	Moderate drought	Severe drought
DSI	2008.05 ~ 2009.01 (9 months)		
	2009.03 ~ 2009.07 (5 months)	2009.02	
	2012.05 ~ 2012.09 (5 months)	2012.12	
	2013.01 ~ 2013.03 (3 months)	2014.09	
	2013.11 ~ 2014.01 (3 months)	2015.08~2015.09	
WSDI	2014.05 ~ 2014.08 (4 months)		
	2015.01 ~ 2015.04 (4 months)		
	2007.10 ~ 2009.01 (16 months)		
	2009.03 ~ 2009.12 (10 months)	2009.02	
	2010.06 ~ 2012.11 (30 months)	2012.12	
SIG	2013.01 ~ 2016.04 (40 months)	2010.03~2010.04	
	2010.02 ~ 2010.06 (5 months)	2013.03	2015.01
	2013.02 ~ 2013.04 (3 months)	2014.09	2015.03
	2014.04 ~ 2014.10 (7 months)	2014.11~2014.12	2015.09
	2015.10 ~ 2016.01 (4 months)	2015.02	
		2015.04~2015.08	

Using GRACE-DSI, GRACE-WSDI, and GRACE-SGI, we analyzed the wet and dry conditions in the past 20 years in Central Asia. Figure 6 demonstrates the change rate of the drought indexes and the MK trend line. Both GRACE-DSI and GRACE-WSDI show a similar spatial change, decreasing in most areas that include Uzbekistan, Kyrgyzstan, Tajikistan, and Western regions Kazakhstan and Turkmenistan. The significant reduction trend in the areas highlights the harsh arid condition and deteriorating trend in Central Asia. Particularly, the arid condition in western Central Asia, the eastern coast of the Caspian Sea, and the Aral Sea basin has deteriorated severely. Studies argued that lasting deterioration is mainly ascribed to human interference [19, 48]. However, the hydrological drought indicators in eastern Kazakhstan and eastern Turkmenistan showed a significant upward trend, indicating that the partial drought condition has been alleviated. Overall, GRACE-SGI is consistent with GRACE-DSI and GRACE-WSDI. However, the trend of GRACE-SGI is different from those of GRACE-DSI and GRACE-WSDI in northwestern Kazakhstan. The GRACE-SGI for the northwest of Kazakhstan increased significantly. The trend indicates that the amount of groundwater resources is increasing in these regions.

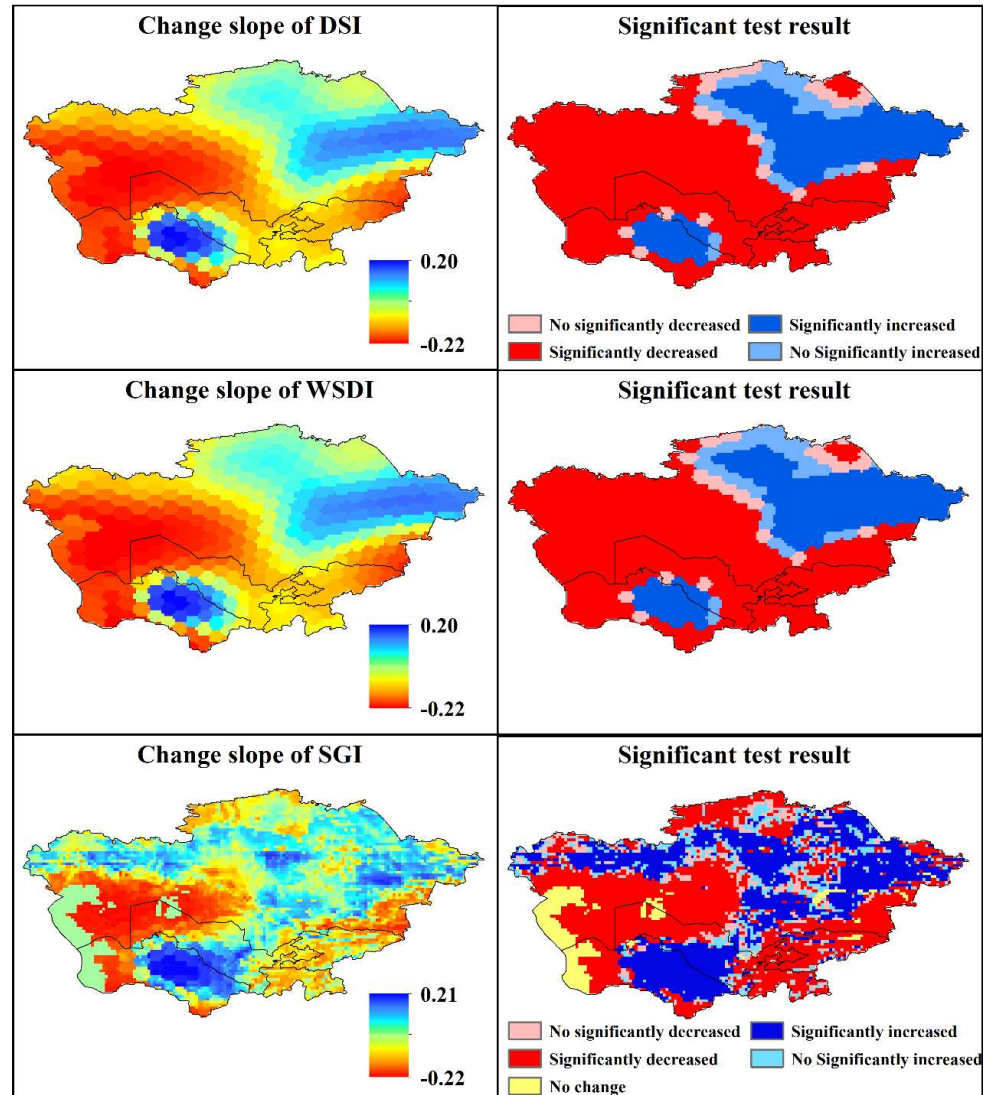


Figure 6. GRACE-DSI, GRACE-WSDI, and GRACE-SGI monthly rate of change and MK significance test results.

3.5. Correlation analysis between drought index and vegetation

The correlation coefficients between the growing season (April-September) NDVI of the Central Asian region from 2002 to 2017 and the GRACE drought indexes of the corresponding months were calculated. According to the correlation coefficients (Fig. 8), the GRACE drought indexes are sensitive to regional water resources and affect the growth of regional vegetation. The correlation coefficients between the drought indexes and NDVI are high during the growing season, especially in the middle of the growing season (July) when the correlation coefficient is the highest. Zhao et al. [31] argued that GRACE-DSI is able to capture the relationship between vegetation-soil water correlation and latitude. Central Asia also exhibits this regular distribution; GRACE-DSI and NDVI in the high latitude regions are mainly positively correlated, while those in low latitudes are mainly negative. The correlation distribution between GRACE-WSDI and NDVI are similar to that between GRACE-DSI and NDVI, while the correlation between GRACE-SGI and NDVI is different from the two above. A comparative analysis found that the correlation coefficient between GRACE-SGI and NDVI during the growing season is mainly negatively correlated. Notably, it has a strong negative correlation in the cultivated land in northern Central Asia from July to September and in the grassland area in northern

Central Asia from June to September, implying decreasing groundwater resources and growing vegetation in this region. Therefore, vegetation growth in the areas depends not only on precipitation but also on groundwater consumption.

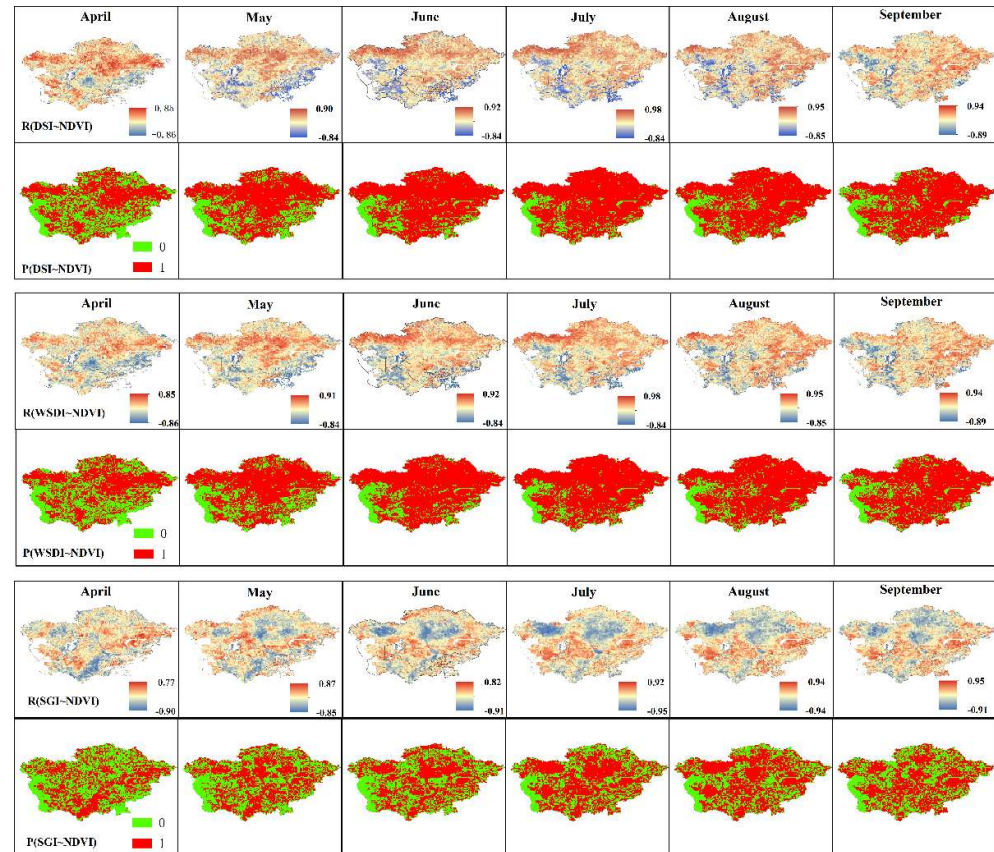


Figure 7. Correlation between the GRACE indicators (i.e., GRACE-DSI, GRACE-WSDI and GRACE-SGI) and the MODIS NDVI for the growing season (April - September).

4. Conclusions

Using the data from the GRACE gravity satellites and MODIS NDVI, we analyzed the hydrological drought and groundwater drought of Central Asia and explored the spatiotemporal characteristics of the arid regional environment and its impact on the surface ecological environment. The main conclusions are as follows:

1) Since the beginning of the 21st century, the annual precipitation in Central Asia increased slightly at a rate of 0.39 mm/year ($p = 0.82$). The temperature increased slightly at a rate of 0.05 °C/year ($p = 0.10$). The water storage decreased at a rate of -0.59 mm/year ($p < 0.01$), and has experienced a decrease-increase-decrease process.

2) The GRACE hydrological drought indicator showed a strong correlation with the traditional drought indicator SPI, which implies the suitability for evaluating long-term comprehensive drought events.

3) The environment in Central Asia was arid from 2007 to 2015 and suffered from various degrees of hydrological and groundwater droughts.

4) Since the beginning of the current century, the arid conditions have deteriorated in Uzbekistan, Kyrgyzstan, Tajikistan, western Kazakhstan, and western Turkmenistan. The drought environment on the eastern coast of the Caspian Sea and the Aral Sea Basin has deteriorated severely.

5) The arid condition affects vegetation growth since vegetation requires extra groundwater resources in such an arid area. During the growing season, the GRACE indexes and NDVI show a significant correlation, while the NDVI of cultivated land and

grassland areas of Central Asia show a significantly negative correlation with the GRACE groundwater drought index.

With the socio-economic development and the promotion of ecological civilization, the need for drought prevention and mitigation is very urgent. Therefore, it is of great significance to improve drought monitoring, prediction, and assessment in order to prevent and reduce the impacts of the droughts. This paper quantitatively assessed the drought dynamics in Central Asia since the beginning of the 21st century by analyzing the GRACE data. The analysis upon spatiotemporal distribution of drought events and the vegetation feedback on drought provides reliable support for understanding and adapting the region's ecological environment.

Author Contributions: Conceptualization, Keting Feng; Data curation, Yanping Cao; Funding acquisition, Yaonan Zhang; Methodology, Keting Feng; Resources, Yongping Shen; Writing – original draft, Keting Feng; Writing – review & editing, Yanping Cao.

Funding: This study was financially supported by the National cryosphere desert data center (E01Z7902), the Capability improvement project for cryosphere desert data center of the Chinese Academy of Sciences (Y9298302) and the National Nature Science Foundation of China (41701503).

Acknowledgments: We thank all the members of National Cryosphere Desert Data Center at Northwest Institute of Eco-Environment and Resources, CAS, who helped and supported our research. We really appreciate the modification and useful amending advice for this manuscript from Dr. Lele Shu and Ling Zhang in Northwest Institute of Eco-Environment and Resources, CAS.

Conflicts of Interest: The authors declare no conflict of interest.

References

1. Yang, P.; Xia, J.; Zhang, Y.; Zhan, C.; Sun, S. How is the risk of hydrological drought in the Tarim River Basin, Northwest China? *The Science of the Total Environment*. **2019**, *693*, 133551-5.
2. Obasi, G. WMO's role in the international decade for natural disaster reduction. *B. Am. Meteorol. Soc.* **1994**, *75*, 1655-61.
3. Pachauri, K.; Meyer, A. CLIMATE CHANGE 2014. SYNTHESIS REPORT. *Environmental Policy Collection*. **2014**, *27*, 408.
4. Solomon, S.D.; Qin, D.; Manning, M.; Chen, Z.; Miller, H.L. Climate Change 2007 : The Physical Science Basis. Working Group I Contribution to the Fourth Assessment Report of the IPCC. *Intergovernmental Panel on Climate Change*. **2007**.
5. Van Loon, A.F.; Gleeson, T.; Clark, J.; Van Dijk, A.I.J.M.; Stahl, K.; Hannaford, J.; Di Baldassarre, G.; Teuling, A.J.; Tallaksen, L.M.; Uijlenhoet, R.; *et al.*. Drought in the Anthropocene. *Nat. Geosci.* **2016**, *9*, 89-91.
6. Omer, A.; Zhuguo, M.; Zheng, Z.; Saleem, F. Natural and anthropogenic influences on the recent droughts in Yellow River Basin, China. *Sci. Total Environ.* **2020**, *704*, 135428.
7. Chen, F.; Huang, W.; Jin, L.; Chen, J.; Wang, J. Spatiotemporal precipitation variations in the arid Central Asia in the context of global warming. *Science China Earth Sciences*. **2011**, *54*, 1812-21.
8. Deng, M.; Long, A.; Zhang, Y.; Xiangquan, L.I.; Lei, Y. Assessment of Water Resources Development and Utilization in the Five Central Asia Countries. *Advances in Earth Science*. **2010**, *25*, 1347-56.
9. Pritchard, H.D. Asia's shrinking glaciers protect large populations from drought stress. *Nature*. **2019**, *569*, 649-54.
10. Lioubimtseva, E.; Cole, R.; Adams, J.M.; Kapustin, G. Impacts of climate and land-cover changes in arid lands of Central Asia. *J. Arid Environ.* **2005**, *62*, 285-308.
11. Puigdefábregas, J. Ecological impacts of global change on drylands and their implications for desertification. *Land Degrad. Dev.* **1998**, *9*, 393-406.
12. Hu, Z.; Zhang, C.; Hu, Q.; Tian, H. Temperature Changes in Central Asia from 1979 to 2011 Based on Multiple Datasets. *J. Climate*. **2014**, *27*, 1143-67.
13. Li, X.; Gao, X.; Chang, Y.; Mu, D.; Liu, H.; Sun, Z.; Guo, J. Water storage variations and their relation to climate factors over Central Asia and surrounding areas over 30 years. *Water Supply*. **2017**, *18*, 1564-80.
14. Deng, H.; Chen, Y. Influences of recent climate change and human activities on water storage variations in Central Asia. *J. Hydrol.* **2017**, *544*, 46-57.
15. Yuan, X.; Wang, W.; Cui, J.; Meng, F.; Kurban, A.; Maeyer, P.D. Vegetation changes and land surface feedbacks drive shifts in local temperatures over Central Asia. *Sci. Rep.-UK*.
16. Zhang, R.; Zhao, C.; Ma, X.; Brindha, K.; Han, Q.; Li, C.; Zhao, X. Projected Spatiotemporal Dynamics of Drought under Global Warming in Central Asia. *Sustainability-Basel*. **2019**, *11*.
17. Guo, H.; Bao, A.; Ndayisaba, F.; Liu, T.; Jiapaer, G.; El-Tantawi, A.M.; De Maeyer, P. Space-time characterization of drought events and their impacts on vegetation in Central Asia. *J. Hydrol.* **2018**, *564*, 1165-78.
18. Dubovyk, O.; Ghazaryan, G.; González, J.; Graw, V.; Löw, F.; Schreier, J. Drought hazard in Kazakhstan in 2000–2016: a remote sensing perspective. *Environ. Monit. Assess.* **2019**, *191*, 510.

19. Jiang, L.; Jiapaer, G.; Bao, A.; Kurban, A.; Guo, H.; Zheng, G.; De Maeyer, P. Monitoring the long-term desertification process and assessing the relative roles of its drivers in Central Asia. *Ecol. Indic.* **2019**, *104*, 195-208.
20. Lioubimtseva, E.; Henebry, G.M. Climate and environmental change in arid Central Asia: Impacts, vulnerability, and adaptations. *J. Arid Environ.* **2009**, *73*, 963-77.
21. Wang, F.; Wang, Z.; Yang, H.; Di, D.; Zhao, Y.; Liang, Q. Utilizing GRACE-based groundwater drought index for drought characterization and teleconnection factors analysis in the North China Plain. *J. Hydrol.* **2020**, *585*, 124849.
22. Hao, Z.; AghaKouchak, A. A Nonparametric Multivariate Multi-Index Drought Monitoring Framework. *J. Hydrometeorol.* **2014**, *15*, 89-101.
23. Tapley, B.D.; Bettadpur, S.; Ries, J.C.; Thompson, P.F.; Watkins, M.M. GRACE Measurements of Mass Variability in the Earth System. *Science*, 305.
24. Cao, Y.; Nan, Z.; Cheng, G.; Zhang, L.; Nelson, B.R. Hydrological Variability in the Arid Region of Northwest China from 2002 to 2013. *Adv. Meteorol.* **2018**, *2018*, 1502472.
25. Long, D.; Scanlon, B.R.; Longuevergne, L.; Sun, A.Y.; Fernando, D.N.; Save, H. GRACE satellite monitoring of large depletion in water storage in response to the 2011 drought in Texas. *Geophys. Res. Lett.* **2013**, *40*, 3395-401.
26. Reyer, C.P.O.; Otto, I.M.; Adams, S.; Albrecht, T.; Baarsch, F.; Cartsburg, M.; Coumou, D.; Eden, A.; Ludi, E.; Marcus, R.; et al.. Climate change impacts in Central Asia and their implications for development. *Reg. Environ. Change.* **2017**, *17*, 1639-50.
27. Zhang, C.; Ren, W. Complex climatic and CO₂ controls on net primary productivity of temperate dryland ecosystems over central Asia during 1980–2014. *Journal of Geophysical Research: Biogeosciences.* **2017**, *122*, 2356-74.
28. Unger-Shayesteh, K.; Vorogushyn, S.; Merz, B.; Frede, H.G. Introduction to “Water in Central Asia – Perspectives under global change”. *Global Planet. Change.* **2013**, *110*, 1-3.
29. Li, Z.; Fang, G.; Chen, Y.; Duan, W.; Mukanov, Y. Agricultural water demands in Central Asia under 1.5 °C and 2.0 °C global warming. *Agr. Water Manage.* **2020**, *231*, 106020.
30. Save, H.; Bettadpur, S.; Tapley, B.D. High-resolution CSR GRACE RL05 mascons. *Journal of Geophysical Research: Solid Earth.* **2016**.
31. Zhao, M.; Velicogna, I.; Kimball, J.S. Satellite observations of regional drought severity in the continental United States using GRACE-based terrestrial water storage changes. *J. Climate.* **2017**, *30*, 6297-308.
32. Yu, W.; Li, Y.; Cao, Y.; Schillerberg, T. Drought Assessment using GRACE Terrestrial Water Storage Deficit in Mongolia from 2002 to 2017. *Water-Sui.* **2019**, *11*, 1301.
33. Cao, Y.; Nan, Z.; Cheng, G. GRACE Gravity Satellite Observations of Terrestrial Water Storage Changes for Drought Characterization in the Arid Land of Northwestern China. *Remote Sens.-Basel.* **2015**, *7*, 1021-47.
34. Hachborn, E.; Berg, A.; Levison, J.; Ambadan, J.T. Sensitivity of GRACE-derived estimates of groundwater-level changes in southern Ontario, Canada. *Hydrogeol. J.* **2017**, *25*, 2391-402.
35. Bloomfield, J.P.; Marchant, B.P. Analysis of groundwater drought building on the standardised precipitation index approach. *Hydrol. Earth Syst. Sci.* **2013**, *17*, 4769-87.
36. Rodell, M.; Houser, P.R.; Jambor, U.; Gottschalck, J.; Bosilovich, M. The global land data assimilation system. *B. Am. Meteorol. Soc.* **2004**, *85*, 381-94.
37. McKee, T.B.; Doesken, N.J.; Kleist, J. The relationship of drought frequency and duration to time scales. Proceedings of the 8th Conference on Applied Climatology, Vol. 17. Boston, MA, American Meteorological Society, 1993,179-83.
38. Döll, P.; Kaspar, F.; Lehner, B. A global hydrological model for deriving water availability indicators: model tuning and validation. *J. Hydrol.* **2003**, *270*, 105-34.
39. Müller Schmied, H.; Eisner, S.; Franz, D.; Wattenbach, M.; Portmann, F.T.; Flörke, M.; Döll, P. Sensitivity of simulated global-scale freshwater fluxes and storages to input data, hydrological model structure, human water use and calibration. *Hydrol. Earth Syst. Sc.* **2014**, *18*, 3511-38.
40. Hayes, M.J.; Svoboda, M.D.; Wihite, D.A.; Vanyarkho, O.V. Monitoring the 1996 Drought Using the Standardized Precipitation Index. *B. Am. Meteorol. Soc.* **1999**, *80*, 429-38.
41. Mishra, A.K.; Singh, V.P. A review of drought concepts. *J. Hydrol.* **2010**, *391*, 202-16.
42. Sinha, D.; Syed, T.H.; Famiglietti, J.S.; Reager, J.T.; Thomas, R.C. Characterizing Drought in India Using GRACE Observations of Terrestrial Water Storage Deficit. *J. Hydrometeorol.* **2017**, *18*, 381-96.
43. Seo, J.Y.; Lee, S. Spatio-Temporal Groundwater Drought Monitoring Using Multi-Satellite Data Based on an Artificial Neural Network. *Water-Sui.* **2019**, *11*, 1953.
44. Li, X.; Lei, S.; Cheng, W.; Liu, F.; Wang, W. Spatio-temporal dynamics of vegetation in Jungar Banner of China during 2000–2017. *J. Arid Land.* **2019**, *11*, 837-54.
45. Liu, Y.; Li, C.; Liu, Z.; Deng, X. Assessment of spatio-temporal variations in vegetation cover in Xinjiang from 1982 to 2013 based on GIMMS-NDVI. *Acta Ecologica Sinica.* **2016**, *36*.
46. Chen, X.; Wang, S.; Hu, Z.; Zhou, Q.; Hu, Q. Spatiotemporal characteristics of seasonal precipitation and their relationships with ENSO in Central Asia during 1901–2013. *J. Geogr. Sci.* **2018**, *28*, 1341-68.
47. Cammalleri, C.; Barbosa, P.; Vogt, J. Analysing the relationship between multiple-timescale SPI and GRACE terrestrial water storage in the framework of drought monitoring. *Water-Sui.* **2019**, *11*, 1672.
48. Jiang, L.; Guli; Jiapaer; Bao, A.; Guo, H.; Ndayisaba, F. Vegetation dynamics and responses to climate change and human activities in Central Asia. *Sci. Total Environ.* **2017**, *599-600*, 967-80.